Proc. CIBSE A: Building Serv. Eng. Res. Technol. **20**(2) 45–50 (1999) Printed in Great Britain B512

Summary Although the power law equation may be used to correlate air flow rate to the pressure difference across a tongue-and-groove floor, the relationship between the coefficient and exponent and the physical parameters of the crack remains concealed to research. Moreover, the pressure loss through the cracks between floorboards of an in-situ floor is reasonably described by the empirical equation for cracks with known dimensions. This is $\Delta P = AQ + BQ^2$ for pressure differences of 0–50 pascals, although the recorded data is for 2–50 pascals. The present results lend support to the published expression for the determination of the theoretical edge effect constant B. However more work is needed in the area of laminar flow through very small, contorted cracks and in the assessment of the crack length. Finally, it is suggested that crackage between floorboards is due to the nature of materials and practices in the construction industry.

Air infiltration through cracks in suspended timber floors

P T McGrath* MSc CEng MInstE, **E Lai†** BSc PhD CEng MIMechE and **M Roche‡** BEng

*Department of Building and Environmental Health, Nottingham Trent University, Burton Street, Nottingham NG1 4BU, UK
†Department of Mechanical and Manufacturing Engineering, Nottingham Trent University, UK
‡Centro Politecnico Superior, Universidad de Zaragoza, Spain

Received 21 May 1998, in final form 26 November 1998

List of Symbols

A	Laminar flow constant of quadratic equation
B	Edge effect constant of quadratic equation
C_1	Constant in power law equation
C_2	Constant in quadratic equation
C_b	Constant described by Baker
d	Crack width (mm)
ID	Internal diameter referred to inlet pipe (mm)
l	Inlet pipe length (mm)
n	Exponent in power law equation
ΔP	Pressure difference (Pa)
Q	Air flow rate ($m^3\ s^{-1}$)
Q_1	Air flow to inlet chamber ($m^3\ s^{-1}$)
Q_{leak1}	Leakage flow, lower chamber ($m^3\ s^{-1}$)
Q_{inf}	Air infiltration from lower to upper chamber ($m^3\ s^{-1}$)
R	Coefficient of correlation
R^2	Coefficient of determination

1 Introduction

Adventitious infiltration of air (infiltration) can cause up to 54% of a dwelling's heat loss[1]. One component of infiltration is air from a basement or sub-floors. An investigation by Lilley *et al.*[2], on a four-bedroom house, using sulphur hexafluoride (SF_6) and nitrous oxide (N_2O) in conjunction with the British Gas ventilation measurement system (AUTOVENT), showed that air from the sub-floor void can contribute up to two thirds of a whole-house ventilation rate. Air from the sub-floor void may also be the transport medium for pollutants from contaminated soils to the living space[3,4].

Several computer models exist to predict whole-house ventilation rates, e.g. BREVENT and COMIS (a multizone model). However, little is known about infiltration from sub-floor voids and basements to the living space. The reason, suggested by Edwards *et al.*[5], for the lack of information is the time-consuming effort required to complete an experiment, as well as difficulty in achieving uniform mixing of the tracer gas on-site. Moreover, their evaluation of BREVENT model (developed by the Building Research Establishment, UK) found that buoyancy effects were more dominant in the sub-floor ventilation rates where wind velocities were less than 1 m s^{-1}. When airflow from the sub-floor to the roof space through the cavity was examined for houses in New Zealand by Basset[6], it was concluded that the predominant airflow through the house is upwards and that no comparative data exist for roofs or sub-floors. Hartless[7] showed that the ventilation rates of sub-floor voids varied between 3 and 13 ac h^{-1} and that there was significant air flow through the cavity between the plasterboard and the wall. Although no indication was given of the precise flow rates , it was suggested that the reason for the high sub-floor void ventilation rates was the open nature of this cavity in conjunction with the stack effect.

McGrath and McManus[8] investigated the air flow from basements and sub-floors into the living space and showed that air flow from basements constitutes a potential nuisance. Using the tracer gas decay technique and focusing on the basement/living space floors of two Victorian houses it was shown that:

(*a*) The floor between the living space and basement provides a major flow path of upward air, and this may contribute significantly to the air change rate in the living space.
(*b*) Cracks between the floorboards and the floor and wall allow significant airflow into the living space from the basement.
(*c*) The basement or sub-floor is a significant source of cold air into a house.

Their work also supports Edwards' assertion that experiments in basement areas are difficult and can cause physical damage to the wall and/or ceiling finishes.

It is accepted that air infiltration is a major source of heat loss in UK housing and that air entering the living space is a potential transport medium for ground contaminants. The lack of published data on airflow from these areas has meant that further research is necessary to quantify the extent of the problem and to deduce a correlation between pressure difference and air flow rate, which could be used for computer modelling. To provide this information, the authors began an investigation to examine air flow through a typical modern suspended wooden floor above a basement or sub-floor.

2 Experiment

The difficulty of conducting experiments on in-situ basements, identified above, defined a need for an experimental rig to be constructed to investigate the nature of air flow through a suspended timber floor. However, the varying condition of many suspended timber floors has meant that one type of floor has to be identified so that its physical properties can be quantified and used in an analysis. The floor type chosen is a typical suspended timber floor that may be found in current housing built using modern construction practice.

2.1 Test rig

The experimental rig was a purpose-built timber chamber that was divided into two 600 mm (height) clear volumes (Figure 1) by a timber floor (12.5 m^{-2}) to simulate the construction over a basement or sub-floor void. The chamber was constructed of 2.4 m × 1.2 m chipboard screwed to supporting timbers. The chamber was internally lined with 1200 g polythene sheeting joined by parcel tape. All the punctures by screws were sealed by silicone sealant. The timber floor was made of new 125 × 25 mm tongue-and-groove floor boarding nailed onto 150 × 50 mm carcassing timber. A 12.5 mm gap was left between the floor perimeter and the wall in accord with normal construction practice. The gap between the floor and the living space wall is normally hidden by a skirting board, which is not intended as an effective seal against air flow. In this study the gap was found to act as free path for air flow and was subsequently stopped with strips of 50 × 25 mm timber, nailed to the floor and sealed with silicone sealant to achieve a near perfect seal for this experiment.

Air flow entered the chamber through a 1000 mm (l) × 105 mm (ID) plastic pipe, that was regulated by a variable-speed centrifugal fan (250 mm) and a damper at the pipe entry point. The mean air velocity through the inlet pipe was determined by means of a Pitot-static tube located 1 m downstream of the entry point, where reasonably developed flow conditions were anticipated, and 100 mm before the pipe exit. Bulk pressure across the floor was measured by an inclined manometer connected to pressure tappings above and below the floor. This enabled pressure differences as low as 1.5 Pa to be recorded.

2.2 Procedure

The purpose of the test was to measure volume flow rate and the corresponding pressure differences across the timber floor over the pressure range 0–50 Pa. This, by convention, is considered to be the upper pressure difference limit for analysing flow through building components. It accords with the Air Infiltration and Ventilation Centre numerical database for building components[9]. A value of 50 Pa is used because it enables data for a building component to be collected and analysed without being affected by atmospheric wind pressure and buoyancy effects. The flow conditions at the measuring station were determined from velocity measurements across the pipe, which revealed a flattened profile similar to that for turbulent flow. It was therefore concluded that air flow at the measuring station would always be fully developed (i.e. turbulent). Consequently, velocity pressures were measured at four equally spaced positions across the pipe and a mean velocity was obtained. The volume flow rate (m^3 s^1) is given by the product of the mean velocity and the cross-sectional area of the pipe.

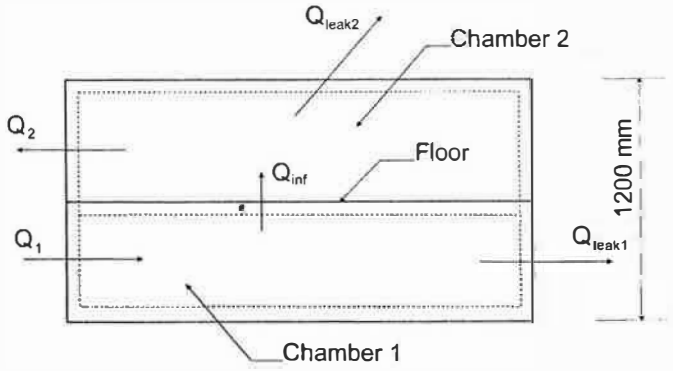

Figure 1 Test rig

Commissioning tests identified considerable leakage through the lid in the upper chamber of the rig. Three flow paths were therefore identified for analysis as follows: airflow through the inlet pipe into the lower chamber (Q_1), leakage airflow in the lower chambers (Q_{leak1}) and airflow through the floor from the lower to the upper chamber (Q_{inf}). Leakage in the lower chamber (Q_{leak1}) was quantified by sealing the floor with a polythene sheet and sealing tape to isolate the lower chamber from the upper chamber. The lower chamber was pressurised and velocity pressure readings were taken through the range 2–50 Pa. The low tube inlet velocities for leakage were recorded using an Alcom hot-wire anemometer. The anemometer readings were compared with those of the Pitot tube for the higher velocities, and the agreement was found to be within 3%. It was therefore assumed that the same accuracy would apply to lower velocities. Because of the large volume of the rig, the maximum pressure difference that could be generated by the fan was 34 Pa at the chamber inlet. The results presented in the next section for 35–50 Pa are therefore extrapolated values.

2.3 Experimental results

The purpose of the investigation is to establish a relationship between the volume flow rate and pressure difference across the floor of the experimental chamber. The initial investigation was confined to studying the flow rates into the lower chamber (Q_1) and the leakage (Q_{leak1}), from which the flow rate across the floor would be calculated. The results were recorded on six separate occasions, three each for the leakage and the inflow into the chamber. The repeatability of the results (Appendix 1) was checked graphically and they were found to agree closely. For convenience, the results are presented as composite plots relating flow rate to pressure difference. The coefficient of determination R^2 was also calculated for the leakage and inflow curves. Values for the floor infiltration curve were calculated by subtracting values of the leakage curve from the inflow curve for coincident pressure differences.

The data was analysed using the following techniques:
(*a*) The power law equation (Figures 2 and 3) of the form

$$Q = C_1 \Delta P^n \quad (1)$$

(*b*) The quadratic equation (Figure 4) of the form

$$\Delta P = AQ + BQ^2 + C_2 \quad (2)$$

where Q is the volume flow rate, ΔP is the pressure difference, n is the exponent, A and B are constants that relate to crack parameters. C_2 is a constant, found by regression analysis, indicating instrument error at zero pressure difference. Because the inlet tube was sealed and the zero setting of the instruments was checked before each set of readings, it was assumed that instrument error would be negligible and it was set at zero for the analysis. The results were analysed for the 2–10 Pa and 2–50 Pa ranges and were fitted by regression analysis (Figures 2–6). The 2–10 Pa pressure difference range has been analysed because it is more representative of the pressure differences experienced across component at normal atmospheric conditions. The quadratic equation was also solved using discrete values of pressure difference to enable a graph of flow rate versus pressure difference to be compared with the power law equation (Figures 5 and 6). The recorded measurements are tabulated in the Appendix[10].

3 Discussion

3.1 Power law equation

The results were initially plotted as a 2–50 Pa power curve where the infiltration appears to behave as two separate straight-line functions that merge with each other between 8 and 11 Pa. Consequently, the power curves are fitted separately for the 2–50 Pa and 2–10 Pa ranges of pressure difference (Figures 2 and 3). Generally, there is a good correlation between the flow rate and pressure difference with coefficients of correlation (R) greater than 0.9 for the curves. The values on the leakage curve at very low pressure, where the hot-wire anemometer was used, do not tend to zero. Consequently, the exponent n of the power law equation for the 2–10 Pa range was found to be 0.35. If the measurements below 5 Pa are ignored, regression analysis shows that the exponent has a value of 0.58 (Figure 6). This value is within the AIVC published range of values for n (between 0.5 and 1.0)[9]. Because of the inherent difficulties associated with the measurement of very low velocities, the low-pressure (< 5 Pa) data for the leakage curve should be viewed with caution. The choice of the value of n (either 0.35 or 0.58) appeared to have little effect on the 0–50 Pa leakage power curve. Analysis of the 2–10 Pa range revealed almost identical values of exponent and coefficient. The difference in calculated flow rates (Table 1) from each expression is 2.9% at 10 Pa and 18% at 50 Pa. Since the results for the 35–50 Pa range were extrapolated values (see also section 2.2), the flow difference quoted at 50 Pa is for information only.

The values of the pressure difference exponent n and coefficient C_1 from the 2–50 Pa curve are 0.6302 and 0.0007 per m^2, respectively, for a floor of 12.5 m^2. These values are significantly different from the median values for timber floors published by the AIVC ($n = 0.74$, $C_1 = 0.15$ per m^2), and reveal calculated differences in flow rate of 22% for the exponent and an order of 10^3 for the coefficient. Informal discussions with the AIVC indicate that the data are privileged information from unpublished work on installed floors. We therefore suggest that the most reasonable and probable reason for the differences is that the AIVC data include flow rates through

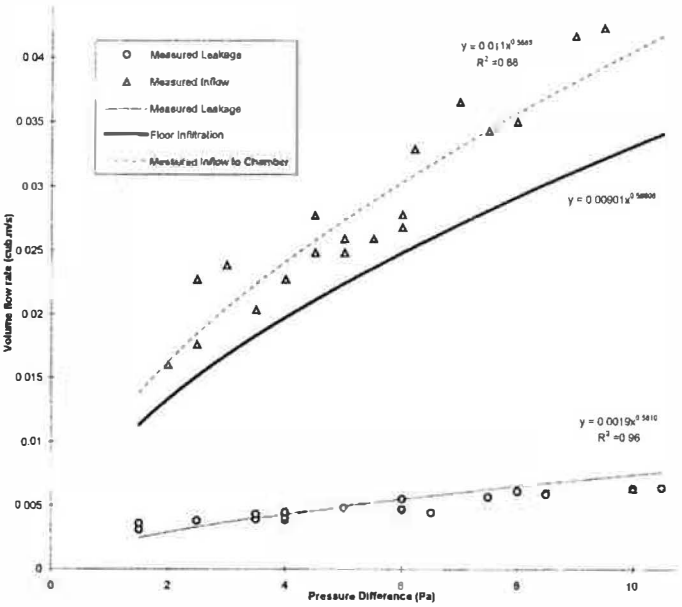

Figure 3 Infiltration versus pressure difference (power curve at 10 Pa)

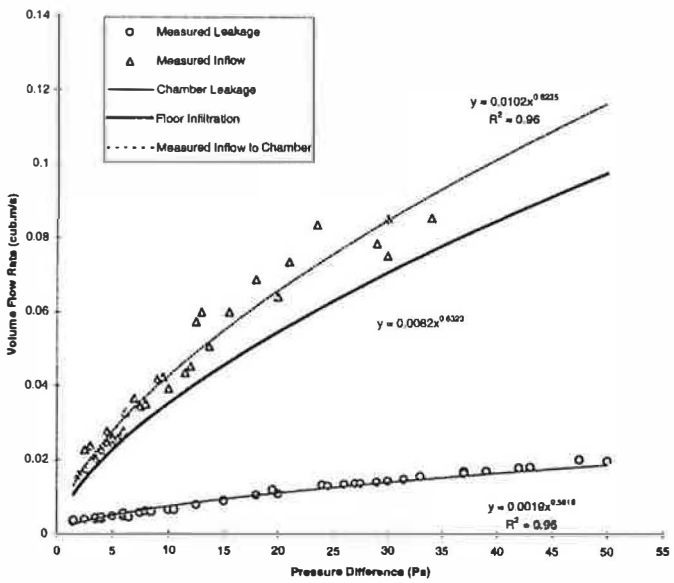

Figure 2 Infiltration versus pressure difference (power curve at 50 Pa)

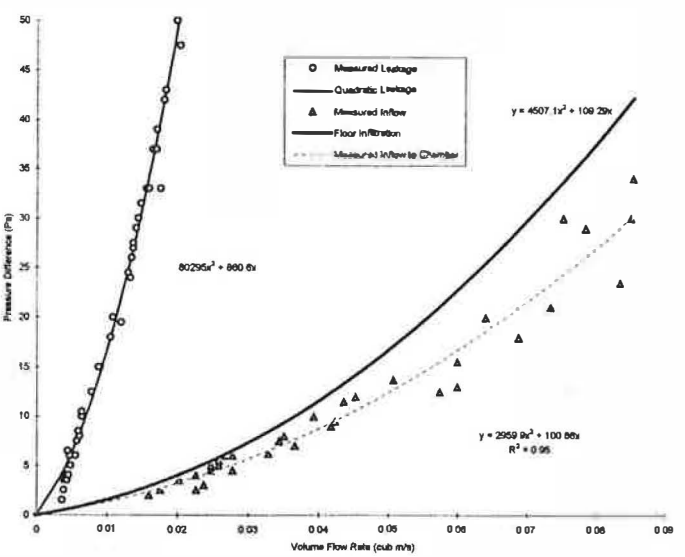

Figure 4 Pressure difference versus infiltration (quadratic curve to 50 Pa)

the gap between the skirting board and floor, whereas the authors values are based on the flow rate, exclusively through the floorboards.

3.2 Quadratic equation

Inspection of Figure 4 suggests that the quadratic equation (equation 2) effectively describes the pressure loss through the floor with coefficients of determination greater than 0.95 for both the leakage and the inflow curves. The leakage data in the 0–5 Pa range are slightly adrift of the quadratic curve, but the resulting error has negligible contribution to the infiltration curve because it is an order of magnitude lower than the infiltration values. When the infiltration quadratic is solved for the flow rate and plotted as function of pressure difference (Figures 5 and 6), the results compare favourably with the power curve, with differences of less than 5% at 5 Pa. However, the apparent lack of generality[11] in determining the coefficient and the exponent of the power curve has meant that another method of data analysis should be investigated when correlating the pressure difference with the flow rate.

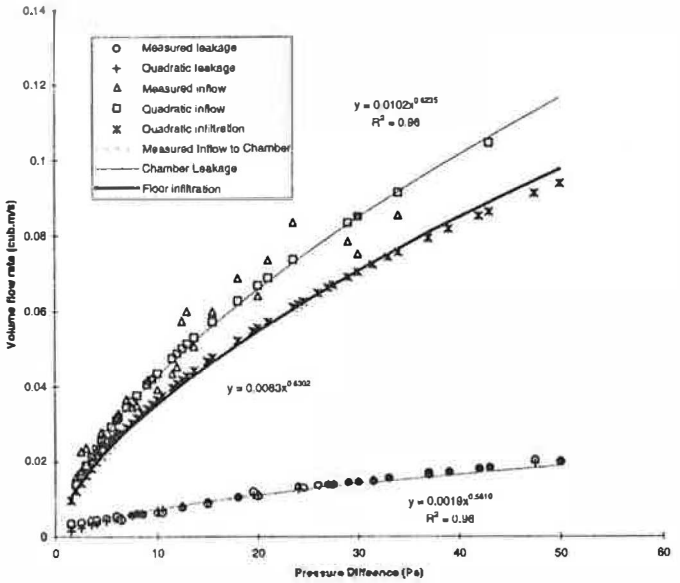

Figure 5 Infiltration versus pressure difference (power curve and quadratic data, 50 Pa)

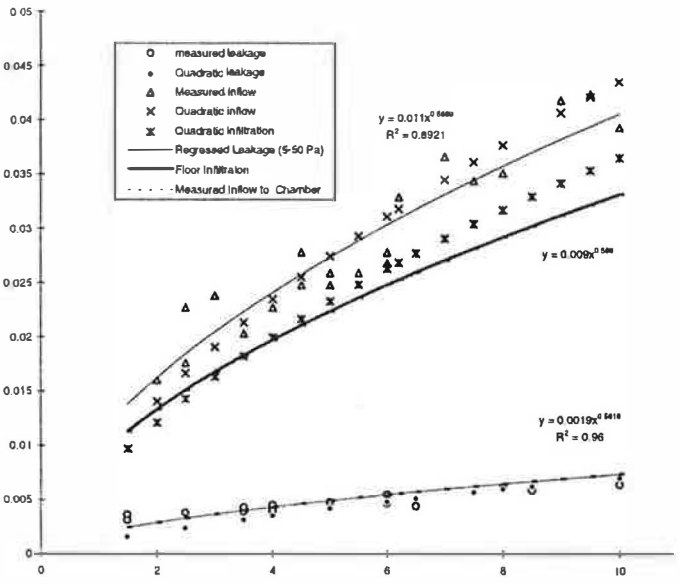

Figure 6 Infiltration versus pressure difference (power curve and quadratic data, 10 Pa)

The airflow through building components described by equation (2) can be considered as made up of two constituent flows : laminar flow (AQ) and flow dominated by edge effects (BQ^2). The theoretical constants A and B may be represented by the following expressions[12]:

Laminar flow:

$$A = 12\mu z/Ld^3 \tag{3}$$

Edge effect:

$$B = \rho C_b/2d^2L^2 \tag{4}$$

where μ is the dynamic viscosity, z is the total distance through the crack, L is the length of the crack as measured on the horizontal plane (in the present study, assumed to be the floorboard length), d is the crack width or thickness, ρ is the air density and C_b is a constant (described by Baker) that relates to the number of bends in the crack. Table 2 compares the values of A and B determined from the regressed data for an estimated crack width of 0.25 mm with those of theoretical analysis. It can be seen that while there is good agreement for the edge effect constant (B), the opposite is true for the laminar flow constant. This suggests that for the present investigation airflow through the floorboards is dominated by edge effects, which are the main contributor to the pressure loss. This may be explained by the fact that airflow through very small cracks in floorboards is subject to interference from surface roughness and/or the turbulence wake after each bend.

For convenience, an assumption has been made in the data analysis that the floorboard length could be used as L in equation (4). This would lead to an underestimation of the theoretical crack depth d and in turn could affect the calculation of the theoretical values of A and B. However, the results (Table 2) yield a reasonable indication of the relative contribution to pressure loss for airflow through the floor, confirmed by good agreement achieved

Table 2 Table of coefficients

Coefficient	Theoretical	From curve
A	3946	109
B	4575	4507

Table 1 Comparison of predicted power curve flow rates

Curve no.	Pressure difference data range (Pa)	Exponent (n)	Constant (c)	Q (10 Pa) ($m^3 s^{-1}$)	Q (50 Pa) ($m^3 s^{-1}$)
i	2–10 Pa.	0.5662	0.0090	0.0344	0.0825
iii	2–50 Pa	0.6302	0.0083	0.0354	0.0977
	Difference against 2–10 Pa data			+2.9%	+18.0%

in the determination of the edge effect constant (B) and the negligible contribution of the laminar flow constant (A).

If the laminar flow constant (A) were solved for the crack width using the regressed data laminar coefficient (109) it would be 0.78 mm. This is highly improbable because the bottom face of the tongue of each floorboard sits on the groove of the adjacent board and a partial seal is formed. However, if the bearing of the floorboard on each rafter is uneven then the seal will be incomplete and gaps will occur. This, in conjunction with expansion and contraction due to the changes in moisture content of the timber, is a contributory factor for large airflow through some floors.

4 Conclusions

(*a*) The power law equation (equation 1) adequately correlates the volume flow rate of air through the floorboards with pressure loss for the 2–50 Pa and 2–10 Pa pressure difference ranges, but lacks generality between the coefficient, the pressure exponent and the crack parameters.
(*b*) The edge effect constant in the quadratic equation determined from the regressed data compares favourably with the results of Baker's work, for an estimated crack width of 0.25 mm, and confirms that edge effects are the major contributor to the pressure loss.
(*c*) The relationship between the pressure loss and volume flow rate through floorboards is closely described by the edge effect term of the quadratic equation (equation 2).
(*d*) The expression, suggested by Baker, for determining the theoretical laminar flow constant of the quadratic equation is not confirmed by this study, and further work is required to ascertain the value of the laminar flow constant for flow through very small cracks.
(*e*) Airflow crackage at timber floor joints is probably due to the uneven nature of the installed floor joists.

References

1 Kendrick J *An overview of combined modelling of heat transport and air movement* Technical Note 40 (Coventry: Air Infiltration and Ventilation Centre) (1993)
2 Lilly J P, Stanaway R J and Biggins J M A study of ventilation characteristics of a suspended floor *Proc. 19th AIVC Conf.* 125–138 (1998)
3 Nazaroff W W and Nero A V *Indoor air passive smoking particulate and housing epidemiology* (Stockholm: Swedish Council for Building Research) (1984)
4 Sieber R, Besant R W and Schoenau G J Indoor air pollutant movement in a single storey house under a range of air circulating conditions *Proc. 5th Jacques Cartier Conf., University of Montreal* (1992)
5 Edwards R, Hartless R and Gaze A Measurement of sub-floor ventilation rates: comparison with BREVENT *Proc. 11th AIVC Conf.* (1990)
6 Basset M R *Infiltration and leakage paths in single family houses — a multi-zone infiltration case study* Technical Note 27 (Coventry: Air Infiltration and Ventilation Centre) (1990)
7 Hartless R and White M K Measuring sub-floor ventilation rates *Proc. 15th AIVC Conf.* (1994)
8 McGrath P T and McManus J Air infiltration from basements and sub-floor to the living space *Building Serv. Eng. Res. Technol.* **17**(2) 85-87 (1996)
9 Orme A S *An analysis and data summary of the AIVC numerical database* Technical Note 44 (Coventry: Air Infiltration and Ventilation Centre) (1994)
10 Roche M *Investigation of infiltration phenomenon at low pressures and calibration of an experimental chamber* BEng Project Report (Dept of Mechanical and Manufacturing Engineering, Nottingham Trent University) (1997)
11 Etheridge D W Crackflow equations and scale effect *Building and Environment* **12**(3) 181–189 (1977)
12 Baker P H, Sharples S and Ward I C Air flow through cracks *Building and Environment* **22**(4) 293–304 (1987)

Appendix

Table 3 Chamber inflow rates ($m^3 s^{-1}$)

Pressure difference (Pa)	Volume flow rate ($m^3 s^{-1}$)
2	0.016
4	0.0227
5	0.0248
5.5	0.0259
6	0.0268
8	0.0351
10	0.0393
12	0.0453
12.5	0.0574
18	0.0688
30	0.0752
34	0.0854

Table 4 Chamber inflow rates ($m^3 s^{-1}$)

Pressure difference (Pa)	Volume flow rate ($m^3 s^{-1}$)
2.5	0.0176
3.5	0.0203
4	0.0227
4.5	0.0248
5	0.0259
6	0.0278
7.5	0.0344
9	0.0418
9.5	0.0424
11.5	0.0436
13.5	0.0507
15.5	0.06
20	0.0641
29	0.0785

Table 5 Chamber inflow rates ($m^3 s^{-1}$)

Pressure difference (Pa)	Volume flow rate ($m^3 s^{-1}$)
2.5	0.0227
3	0.0238
4.5	0.0278
6.0	0.0329
7	0.0366
9	0.0418
13	0.0600
21	0.0735
23.5	0.0835
30	0.0851

Table 6 Leakage flow rates ($m^3 s^{-1}$)

Pressure difference (Pa)	Volume flow rate ($m^3 s^{-1}$)
1.5	0.0031
4	0.0039
6	0.0047
8.5	0.0060
10	0.0064
12.5	0.0078
18	0.0105
26	0.0135
29	0.0141
33	0.0156
37	0.0170
43	0.0183
55	0.0204

Table 7 Leakage flow rates ($m^3 s^{-1}$)

Pressure difference (Pa)	Volume flow rate ($m^3 s^{-1}$)
2.5	0.0038
3.5	0.0039
4	0.0041
6.5	0.0044
8	0.0061
10	0.0064
15	0.0090
19.5	0.0120
24.5	0.0130
27.5	0.0137
31.5	0.0148
39	0.0171
47.5	0.01203

Table 8 Leakage flow rates ($m^3 s^{-1}$)

Pressure difference (Pa)	Volume flow rate ($m^3 s^{-1}$)
1.5	0.0036
3.5	0.0043
4	0.0045
5	0.0048
6	0.0055
7.5	0.0057
8.5	0.0059
10.5	0.0064
15	0.0088
20	0.0108
24	0.0133
27	0.0137
30	0.0144
37	0.0160.
42	0.0181
50	0.0199